Available online at www.sciencedirect.com
ScienceDirect
Nuclear Instruments and Methods in Physics Research B 256 (2007) 547–553
NIM B
Beam Interactions with Materials & Atoms
www.elsevier.com/locate/nimb

A Monte Carlo study of energy deposition at the sub-cellular level for application to targeted radionuclide therapy with low-energy electron emitters

D. Emfietzoglou [a], C. Bousis [a], C. Hindorf [b], A. Fotopoulos [c], A. Pathak [d], K. Kostarelos [e,*]

[a] Medical Physics Laboratory, University of Ioannina Medical School, Ioannina 451 10, Greece
[b] Joint Department of Physics, The Royal Marsden Hospital and Institute of Cancer Research, Sutton, Surrey SM2 5PT, United Kingdom
[c] Department of Nuclear Medicine, University of Ioannina Medical School, Ioannina 451 10, Greece
[d] School of Physics, University of Hyderabad, Hyderabad 500 046, India
[e] Nanomedicine Laboratory, Centre for Drug Delivery Research, School of Pharmacy, University of London, London WC1N 1AX, United Kingdom

Available online 16 December 2006

Abstract

Optimizing targeted radionuclide therapy for patients with circulating malignant cells (e.g. blood-related cancers) or a micrometastatic spread requires quantification of various dosimetric parameters at the single-cell level. We present results on the energy deposition of monoenergetic electrons of initial energy from 100 eV to 20 keV – relevant to Auger emitting radionuclides – distributed either uniformly or at the surface of spherical volumes of radii from 10 nm to 1 μm which correspond to critical sub-cellular targets. Calculations have been carried out by our detailed-history Monte Carlo (MC) code which simulates event-by-event the complete slowing down (to 1 Ry) of both the primary and all subsequent generations of electrons, as well as, by the continuous-slowing-down-approximation (CSDA) using analytic range-energy relationships. The latter method has been adopted by the MIRD committee of the Society of Nuclear Medicine for dosimetry at the cellular level (>1 μm). Differences between the MC and CSDA results are up to ~50% and are expected to be even larger at higher energies and/or smaller volumes. They are attributed to the deficiencies of the CSDA method associated with the neglect of straggling and δ-ray transport. The results are particularly relevant to targeted radiotherapy at the genome level by Auger emitters.

Keywords: Monte Carlo; Cellular dosimetry; Targeted radiotherapy

1. Introduction

The ultimate goal of any radiation therapy modality is to deliver a sterilizing radiation dose to all cancer cells in the body while sparing distant and/or nearby healthy cells [1]. For disseminated disease which exhibits single cells or clusters of cells in the circulation conventional external beam (wide-field) irradiation by high-energy photons or electrons is unlikely to provide an optimum treatment modality due to excess scattering which may result in an unacceptable radiation burden to healthy tissues [1]. Targeted radionuclide therapy (TRT) whereby short-range charged particles (currently mostly electrons) are delivered to cancer cells by radiolabelled tumour targeting agents appears to be the method of choice for micrometastatic and disseminated diseases [2]. However, for TRT to be successful various physical, physiological and biological parameters have to be carefully studied in order to optimise the choice of the radionuclide and its carrier agent [3]. For example, the poor ability of most carriers to penetrate in sufficient quantities into solid tumors has led to the use of intermediate- and high-energy β-emitters (most notable

* Corresponding author. Tel.: +44 207 753 5861; fax: +44 207 753 5942.
E-mail address: kostas.kostarelos@pharmacy.ac.uk (K. Kostarelos).

0168-583X/$ - see front matter © 2007 Elsevier B.V. All rights reserved.
doi:10.1016/j.nimb.2006.12.055

^{90}Y and ^{131}I), with typical ranges spanning several cell diameters, which are capable of effectively cross-irradiating tumor cell populations that are not directly targeted by the radiopharmaceutical [4,5].

After almost 30 years of research in TRT, there is currently increased enthusiasm due to the recent approval (in 2002 and 2003, respectively) of the first two radiopharmaceuticals for TRT of (Non-Hodgkin's) lymphomas; namely, Zevalin® (IDEC Pharmaceuticals, San Diego, CA and Schering AG, Berlin) and Bexxar® (GlaxoSmithKlein, Philadelphia, PA), while several more radiopharmaceuticals are under clinical trials [6,7]. A puzzling finding however, is the fact that despite the significantly higher remission rates compared to the unlabelled drug, the duration of remission was not longer [8,9]. Theoretically, such finding may be explained by the non-optimal relationship between the range of the emitted electrons and the tumor dimensions [10]. Specifically, many lymphoma patients have microscopic disease and almost all patients diagnosed with the most common type of lymphoma, chronic lymphatic leukaemia (CLL; that makes up ~25% of all lymphoma patients), have lots of single tumor cells circulating in blood [11]. Thus, it is not unusual for lymphoma patients to have tumors that may range in size from more than 1 l down to the volume of a single cell. Zevalin uses an antibody labelled with ^{90}Y, a long-range electron-emitter with maximum β energy at 2.28 MeV and maximum range in water 11 mm and Bexxar an antibody labelled with ^{131}I, a medium range electron-emitter with maximum β energy at 0.606 MeV and maximum range in water 2.3 mm. As a result, both radiopharmaceuticals emit electrons that may span several cell diameters (typical cell diameter ~10 μm) resulting in the under-irradiation (perhaps below sterilizing levels) of targeted tumor cells as well as a significant irradiation of nearby healthy cells which may turn malignant later on. A clinical observation compatible with the latter is that of Kaminski et al. [12] that relapse often solely occurs in sites not previously known to be involved with lymphomas.

Today, the dosimetric techniques employed in TRT treatments are usable at the macroscopic level of tissues and organs (mm to cm). It has become clear however, that the optimum efficacy of TRT for tumour cells circulating in blood (or for micrometastatic tumors) requires knowledge of energy deposition at the single-cell level with emphasis on sub-cellular critical structures, such as, for example, the cell nucleus, the chromosome, or the DNA (~nm–μm) [5,13,14].

The aim of the present study is to quantify the energy deposition by low-energy electrons (100 eV–20 keV) distributed either uniformly or at the surface of sub-cellular volumes of various sizes (radius 10–1000 nm). The present energy range is most relevant to Auger emitting radionuclides, while the spatial scale considered corresponds to critical targets (e.g. DNA, chromosome and cell nucleus) for the survival of the cell. Calculations have been carried out by our detailed-history Monte Carlo code [15], as well as, by the continuous-slowing-down-approximation using analytic range-energy relationships. The latter approach has been adopted by the MIRD (Medical Internal Radiation Dose) committee of the Society of Nuclear Medicine [16].

2. Methodology

The absorbed dose, D, defined as the mean energy imparted to matter by ionizing radiation per unit mass, is the central quantity for assessing and predicting the efficacy of any radiotherapeutic modality [3]. Although in some circumstances (e.g. high LET particles) correction factors accounting for the different radiobiological effectiveness between different radiation types may be necessary, the calculation of D still remains the important first step towards any risk-benefit analysis [17]. The standard approach for absorbed dose calculations for internally distributed radionuclides, makes use of the so-called MIRD scheme [3]. This is a conceptually simple mathematical formalism which, with some restrictions, may be applied to any spatial scale of interest, i.e. at both the tissue and cell level [18,19]. Within this formalism the (spatial) mean absorbed dose to a target region r_k from radioactivity in a source region r_h is given by the product:

$$\overline{D}(r_k \leftarrow r_h) = \tilde{A}_h S(r_k \leftarrow r_h), \tag{1}$$

where $\tilde{A}_h$ is the cumulated activity in the source region r_h (i.e. the total number of nuclear disintegrations that take place within r_h) and S is the absorbed dose in the target region r_k per disintegration in the source region r_h. Thus, although $\tilde{A}_h$ may depend on various physiological and biological factors related to the kinetics of the radiopharmaceutical within the body, the S value is a purely physical quantity related to the type and transport properties of the radiation as well as the geometry of the source and target regions. Importantly, calculation of S values may proceed irrespective of any knowledge on $\tilde{A}_h$.

The MIRD committee has provided extensive tabulations of S values from the organ down to the cellular level for a variety of radionuclides and monoenergetic photons and electrons [14]. At the macroscopic level of organs and tissues (mm to cm) S values have been mostly calculated by general-purpose condensed-history Monte Carlo codes, such as, ETRAN, EGS and MCNP [20]. In contrast to other methodologies (e.g. Boltzmann equation), such codes may account in a straightforward manner for the inhomogeneities of the human body as well as the variety of source-to-target geometries encountered in practice. However, the use of such codes is fundamentally unsuitable for the cellular and sub-cellular level since the spatial resolution dictated by their adopted energy cut-off (~1–10 keV electrons) exceeds (or is comparable to) the dimensions of the targets of interest (nm to μm). Thus, the MIRD committee has adopted a deterministic approach to calculate cellular S values based on Cole's [21] analytic range-energy relationships for electrons (or its modification by Howell

et al. [22]) and the application of the (straight-ahead) continuous-slowing-down-approximation (CSDA) [16]. The latter assumes that the primary's particle energy-loss (potential and kinetic energy) from inelastic collisions is deposited at a continuous rate (given by the collision stopping power) along a straight-line trajectory. Importantly, for the present context, the CSDA assigns zero range to all secondary electrons. Within this framework the S value is obtained by [16]:

$$\phi_i(r_k \leftarrow r_h) = \int \Psi_{r_k \leftarrow r_h}(x) \frac{1}{E_i} \frac{\mathrm{d}E}{\mathrm{d}X}\bigg|_{X(E_i)-x} \mathrm{d}x, \tag{2}$$

$$S(r_k \leftarrow r_h) = \sum_i \frac{\Delta_i \phi_i(r_k \leftarrow r_h)}{m_k}, \tag{3}$$

where $\phi_i(r_k \leftarrow r_h)$ is the fraction of energy emitted from the source region that is absorbed in the target region for the ith radiation component (i.e. type and energy), $\Psi_{r_k \leftarrow r_h}(x)$ is the geometric factor representing the mean probability that a randomly directed vector of length x starts from a random point within the source region and ends within the target region, $\mathrm{d}E/\mathrm{d}X|_{X(E_i)-x}$ is an "effective" stopping power (see below) evaluated at $X(E_i) - x$ which is the residual range of a particle with initial energy E_i after passing distance x through the medium, Δ_i is the mean energy of the ith radiation component and m_k is the mass of the target region. Note that, contrary to the organ level, the contribution of photons to the cellular S values may be safely neglected. The MIRD committee makes use of Cole's empirical range-energy expression for $X = f(E)$ which, after inversion to $E = f(X)$ and differentiation provides the effective stopping power, $\mathrm{d}E/\mathrm{d}X$, to be used in Eq. (2). (The term "effective" is used here to denote that the precise interpretation of $\mathrm{d}E/\mathrm{d}X$ depends on which exactly measure of range X represents; this is discussed further below in relation to Fig. 1.) In a series of recent papers [23–25] we have used the MIRD methodology with MC- and CSDA-obtained S values to calculate dose distributions in human organs, micrometastatic tumor spheroids and single-cells and have assessed the efficacy of different carrier modalities and radionuclides.

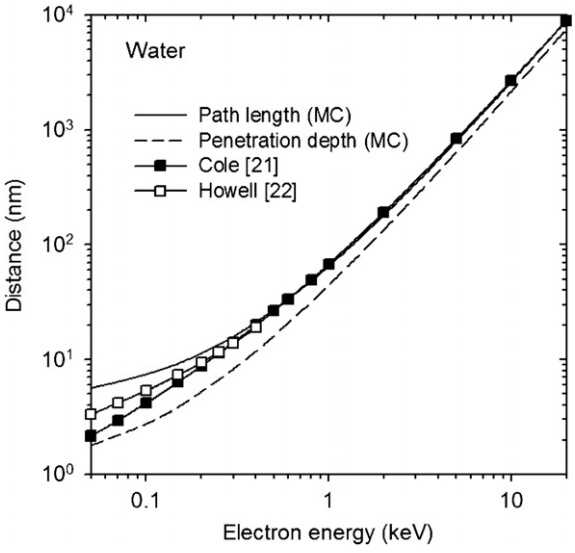

Fig. 1. A comparison between MC calculated path lengths and penetration depths of electrons in a unit density water medium and the analytic formulae of Cole and Howell et al. obtained empirically from experimental data in air and in plastics.

However, the extension of the above CSDA methodology from the cellular (several microns) to the sub-cellular (nm–μm) level becomes problematic since the "discrete" nature of the energy loss process associated with straggling, angular deflections and the finite range of the secondary electrons (hereafter called δ-rays) cannot be neglected at this scale. Detailed-history MC codes simulating event-by-event the slowing down process of all generations of particles are best suited for such applications since they methodologically account for all the above deficiencies of the CSDA. It should be noted that the general-purpose condensed-history MC codes (e.g. EGS, MCNP, ITS, GEANT) are not suitable for application at the sub-cellular level since their spatial resolution for electron transport exceeds ~1 μm. In the present work we use our in-house detailed-history MC code [15] to simulate stochastic tracks of electrons with initial energies from 100 eV to 20 keV in a unit density water medium (electron cut-off = 1 Ry). The cross-section models employed in the present simulations have been described in detail elsewhere [15,26]. In brief, inelastic interactions are described by a two-term Bethe asymptotic expression with parameters adjusted to experimental data for water to obtain the complete (i.e. both the soft and hard component) secondary electron spectrum from each ionization shell of water as well as the discrete excitation probabilities. For elastic scattering we use the screened-Rutherford formula with empirical modifications. In general, efforts have been made to construct differential and total cross-sections in good agreement with all the available experimental data for water. Since the experimental cross-section data are generally accurate to no better than 10%, an indirect test for the consistency of our inelastic cross-section model is provided by the stopping power values which have to approach the predictions of the Bethe formula at ~10 keV (and above). Calculation of stopping power values from the first moment of our differential cross-section for energy loss agrees to within few % with the ICRU recommended values at 10–20 keV.

The simulation results presented are average values over ~10 000 primary electrons. Their overall (statistical) uncertainty is estimated to be less than 5%. For modeling a uniform distribution of radioactivity the point of origin for each primary electron was distributed randomly (proportional to the volume mass) inside the sphere, whereas for a surface distribution the point of origin was restricted at the periphery of the sphere. We consider sphere volumes of 10, 50, 100 and 1000 nm radius which are relevant to critical sub-cellular targets ranging from the DNA to the cell nucleus level.

3. Results and discussion

Fig. 1 presents our MC-calculated range of electrons in a unit density water medium along with the predictions of Cole's [21] empirical formula with and without the low-energy modification (<0.4 keV) of Howell et al. [22]. The path length denotes the crooked path that characterizes the trajectory of electrons in matter whereas the penetration depth denotes the length of the straight-line between the initial and most distant interaction point of the track. Thus, the path length is most closely related to the integral over the reciprocal of the stopping power, whereas the penetration depth to the transmission probability from a spherical geometry. For most of the energy range depicted, the analytic formulae seem to better represent the MC-calculated path length instead of the penetration depth. The difference between the analytic results and the MC-calculated penetration depth is at the 10%–40% level. It is important to recognize that the effective stopping power under the straight-ahead approximation should reflect the penetration depth and not the path length. The mathematical manifestation of the above is that the integral in Eq. (2) is over a (linear) distance across the medium (dx) and not a distance along the particle track; thus, X should be a measure of the penetration depth and not the path length. It follows in Fig. 1 that, under the straight-ahead approximation, Cole's (or Howell's) effective stopping power will underestimate the energy loss calculated by the MC code.

Fig. 2 compares sub-cellular S values by the MC and CSDA methods for a uniform distribution of activity in various spherical volumes. Assuming zero activity in other cell compartments, these S values represent the self-dose component ($r_h \equiv r_k$); for the present energy range, the cross-dose (from other cells) is either zero or, generally, very small. The decrease of the S value by almost an order of magnitude between the sphere volumes depicted is almost solely due to the inverse proportionality of the absorbed dose with the target mass (see Eqs. (1) and (3)) which, in turn, is proportional to r^3 (the absorbed fraction differences between the spheres are well too smaller; see Fig. 4). Although there exists good evidence that DNA-related volumes (<10–100 nm) represent the most important cellular targets, the actual choice of the target volume for dosimetric calculations will depend on the penetration

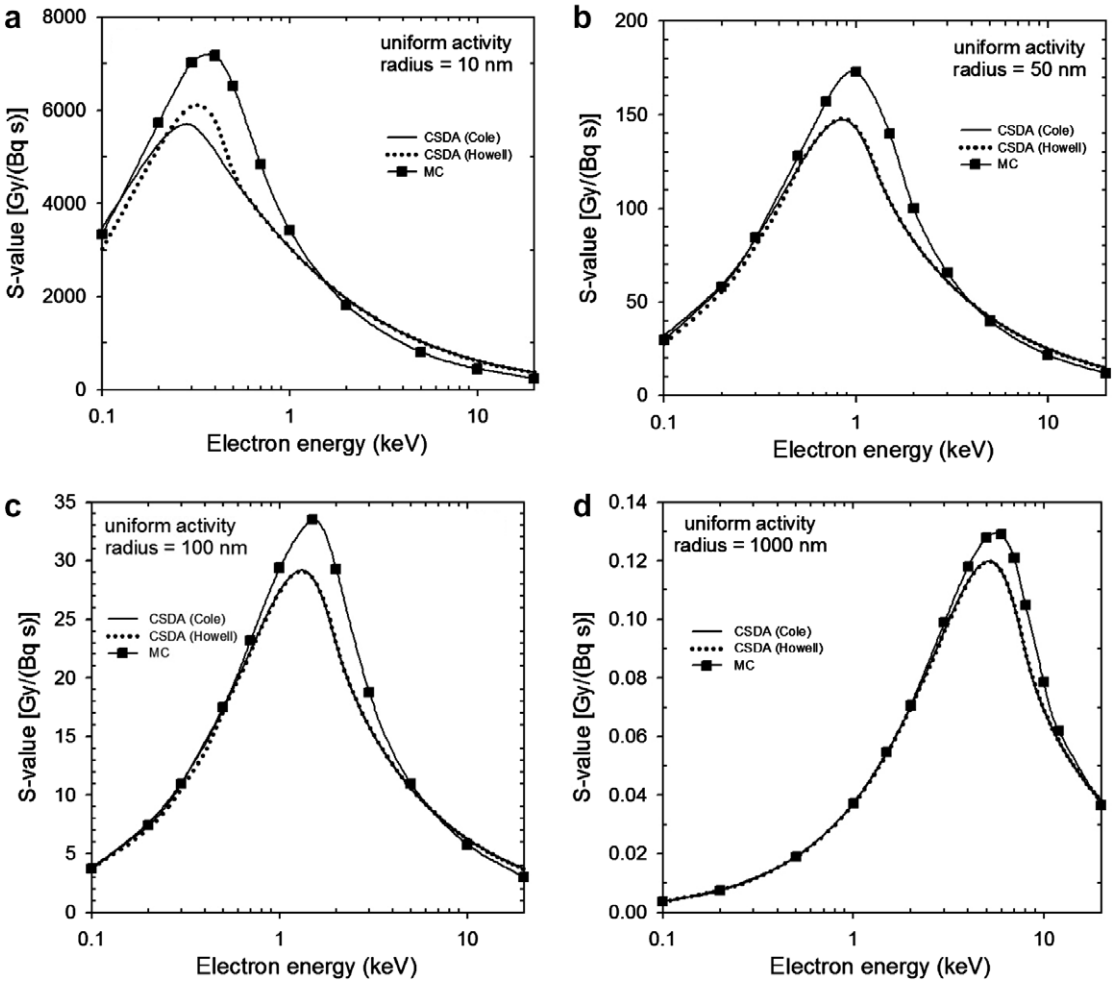

Fig. 2. A comparison of MC and CSDA calculated S values for a uniform distribution of primary electrons in spherical volumes of radii: (a) 10 nm, (b) 50 nm, (c) 100 nm and (d) 1000 nm.

capabilities of the radiopharmaceutical as well as. For example, for radionuclides that do indeed reach the cell nucleus or the DNA, the dosimetry must involve sub-nuclear (i.e. sub-micron) volumes to avoid possible underestimation if averaged over a larger and, perhaps, less biologically relevant volume. The CSDA calculations are based on Eqs. (2) and (3) where the effective stopping power is obtained by differentiation of the analytic range-energy formulae of Cole and Howell et al. The analytic form of the geometric factor Ψ is obtained from [16]. Except for the smallest sphere (panel a) the low-energy modification to Cole's original formula by Howell et al. has a negligible effect since it applies to electrons below 400 eV which have a penetration depth of less than 10 nm (see Fig. 1). Differences between the MC and CSDA results increase with decreasing sphere dimensions. Also, as the sphere increases in size, the maximum difference shifts at higher electron energies.

The above are more clearly depicted in Fig. 3 where we present the S value difference between the MC and the CSDA (Cole) results for both a uniform and a surface activity distribution. The magnitude of the difference is the same for both activity distributions examined. In connection to Fig. 1 we observe that when the electron penetration depth becomes comparable to the sphere radius, the CSDA results underestimate the MC calculations by as much as 20–50%. This difference may be attributed to the overestimation of the MC penetration depth by the CSDA formulae (see discussion above for Fig. 1) which predict that a larger fraction of the primary electron energy will be deposited outside the sphere. In contrast, at high energies the CSDA results progressively overestimate the MC calculations by 10–40%. The reason being that, in the CSDA calculations the escape of energetic δ-rays from the volume is neglected (i.e. their energy is assumed to be deposited along the primary particle track). The importance of this effect is expected to be further enhanced above 20 keV since, with increasing primary electron energy more and more secondaries will be capable of leaving the volume. It therefore appears that differences between the

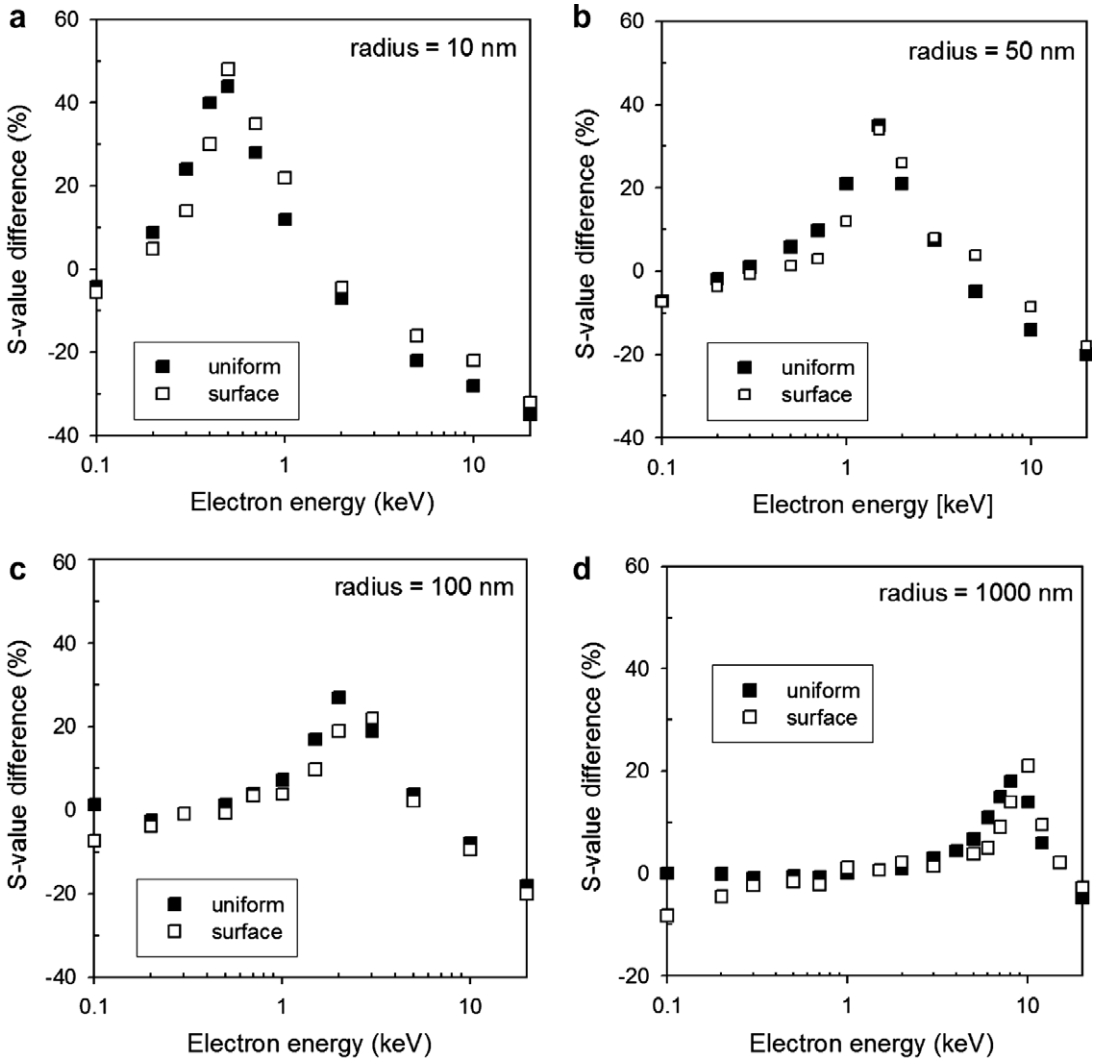

Fig. 3. The S value difference between the MC and CSDA (Cole) results for a uniform and a surface distribution of primary electrons in spherical volumes of radii: (a) 10 nm, (b) 50 nm, (c) 100 nm and (d) 1000 nm.

present MC and CSDA results at low-energies are mainly due to a different account of the primary electron, whereas those at high energies to the different account of the secondaries. The magnitude of the present differences seems to question the assumed adequacy of the (straight-ahead) CSDA approach down to 10 nm spheres [22]. In general, the account of the discrete nature of interactions by the MC method should naturally lead to more accurate estimates of energy deposition than the CSDA for target volumes comparable to or smaller than the range of primary and/or secondary particles. However, the cross-section input is a critical component in any MC code; this is especially true for low-energy electron transport and nanometer-size volumes. Re-evaluation of the present calculations with an improved set of inelastic cross-sections [27,28] is currently in progress.

Fig. 4 presents the absorbed fraction in spheres of 10, 50, 100 and 1000 nm radius for both a uniform and a surface distribution of activity. In contrast to the uniform case, where for sufficiently large volumes and/or low-electron energies the absorbed fraction approaches unity (100% absorption), for a surface distribution the absorbed fraction never exceeds ~50% due to the isotropic emission of the primary particles. Thus, under non-equilibrium conditions and for non-internalized emitter in relation to the targets considered here, the absorbed dose is far from what would have been obtained under the simplistic (and often used) assumption of complete absorption. Interestingly, even for a uniform distribution (perfectly internalized emitter), if the volume is comparable in size to, say, the DNA or the chromatin fiber (<100 nm), most of the energy of primary electrons exceeding ~1 keV will escape.

The above have important implications for the optimum radiolabelling and dosimetry of carriers which are supposed to reach the cell nucleus and target specific sites of the genome [29,30]. Auger emitters (i.e. radionuclides that decay by electron capture or internal conversion) are generally assumed to be most appropriate for labeling carriers

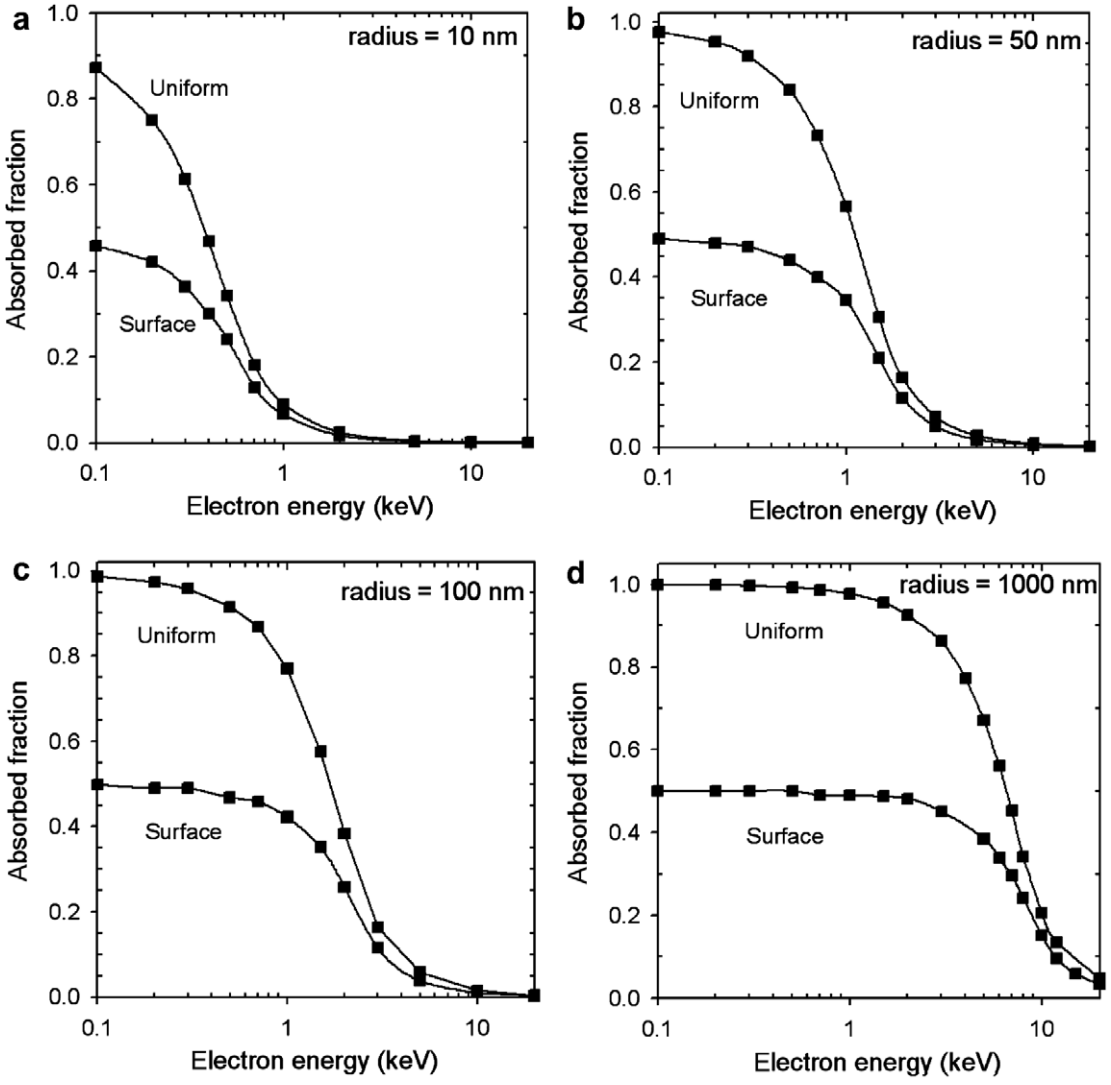

Fig. 4. The MC calculated energy fraction for a uniform and a surface distribution of primary electrons that is absorbed in spherical volumes of radii: (a) 10 nm, (b) 50 nm, (c) 100 nm and (d) 1000 nm.

that are capable of reaching the DNA due to their short irradiation range [21–33]. Despite their relatively large mean energy of emission (typical well above 1 keV) the majority of Auger electrons are below ~500 eV having penetration distances less than ~10 nm [33]. Thus, apart from the requirement of targeting all tumor cells (due to the absence of cross-irradiation effects) the dosimetry of Auger-emitting radiopharmaceuticals is not straightforward since the determination of the most relevant target volume and the intracellular location where the Auger decays occur become critical. As it is evident in Fig. 4, if the target is associated with cellular structures much below the cell nucleus level, the absorbed fraction versus electron energy curve exhibits a steep fall-off at the range of energies directly relevant to the Auger spectra. This may lead to a significant under- or over-estimation of the absorbed dose if unrealistic assumptions are adopted relevant to the target dimensions, the Auger position, or, the exact Auger spectrum. The above are also relevant to an accurate determination of the radiation burden of diagnostic procedures in nuclear medicine and to their risk-benefit analysis, since about 90% of the radionuclides used in such procedures emit Auger electrons [34].

Acknowledgement

This work was partly supported by the United Kingdom Department of Trade and Industry (DTI) (Grant QCBB/013/00057).

References

[1] M.N. Gaze, Phys. Med. Biol. 41 (1996) 1895.
[2] T.E. Wheldon, Phys. Med. Biol. 45 (2000) 77.
[3] G. Sgouros, J. Nucl. Med. 46 (2005) 18.
[4] R.F. Meredith, T.K. Johnson, G. Plott, D.J. Macey, R.L. Vessella, L.A. Wilson, H.B. Breitz, L.E. Williams, Med. Phys. 20 (1993) 583.
[5] J.A. O'Donoghue, M. Bardiès, T.E. Wheldon, J. Nucl. Med. 36 (1995) 1902.
[6] D.E. Milenic, E.D. Brady, M.W. Brechbiel, Nat. Rev. 3 (2004) 488.
[7] B. Brans, O. Linden, F. Giammarile, J. Tennvall, C. Punt, Eur. J. Cancer 42 (2006) 994.
[8] T.E. Witzig, L.I. Gordon, F. Cabanillas, M.S. Czuczman, C. Emmanouilides, R. Joyce, et al., J. Clin. Oncol. 20 (2002) 2453.
[9] A.J. Grillo-López, B.D. Cheson, S.J. Horning, B.A. Peterson, W.D. Carter, C.L. Varns, et al., Ann. Oncol. 11 (2000) 399.
[10] J.L. Humm, J. Nucl. Med. 27 (1986) 405.
[11] A. Johnson, E. Cavallin-Ståhl, M. Åkerman, Br. J. Cancer 52 (1985) 159.
[12] M.S. Kaminski, K.R. Zasadny, I.R. Francis, M.C. Fenner, C.W. Ross, A.W. Milk, et al., J. Clin. Oncol. 14 (1996) 1974.
[13] J.L. Humm, J.C. Roeske, D.R. Fisher, G.T.Y. Chen, Med. Phys. 20 (1993) 535.
[14] M. Bardies, M.J. Myers, Phys. Med. Biol. 41 (1996) 1941.
[15] D. Emfietzoglou, G. Papamichael, K. Kostarelos, M. Moscovitch, Phys. Med. Biol. 45 (2000) 3171.
[16] S.M. Goddu, R.W. Howell, L.G. Bouchet, W.E. Bolch, D.V. Rao, MIRD cellular *S* values, Society of Nuclear Medicine, Reston, VA, 1997.
[17] P.B. Zanzonico, J. Nucl. Med. 41 (2000) 297.
[18] R.W. Howell, J. Nucl. Med. 35 (1994) 531.
[19] A.I. Kassis, J. Nucl. Med. 33 (1992) 781.
[20] M.G. Stabin, M.W. Konijnenberg, J. Nucl. Med. 41 (2000) 149.
[21] A. Cole, Radiat. Res. 38 (1969) 7.
[22] R.W. Howell, D.V. Rao, K.S.R. Sastry, Med. Phys. 16 (1989) 66.
[23] D. Emfietzoglou, K. Kostarelos, G. Sgouros, J. Nucl. Med. 42 (2001) 499.
[24] D. Emfietzoglou, K. Kostarelos, A. Papakostas, W.-H. Yang, A. Ballangrud, H. Song, G. Sgouros, J. Nucl. Med. 46 (2005) 89.
[25] C. Hindorf, D. Emfietzoglou, O. Linden, K. Kostarelos, S.-E. Strand, Cancer Biother. Radiopharm. 20 (2005) 224.
[26] D. Emfietzoglou, G. Papamichael, M. Moscovitch, J. Phys. D: Appl. Phys. 33 (2000) 932.
[27] D. Emfietzoglou, H. Nikjoo, Radiat. Res. 163 (2005) 98.
[28] D. Emfietzoglou, F.A. Cucinotta, H. Nikjoo, Radiat. Res. 164 (2005) 202.
[29] K.J.A. Kairemo, A.P. Jekunen, M. Tenhunen, Gene Ther. Mol. Biol. 4 (1999) 171.
[30] I.G. Panyutin, R.D. Neumann, Trends Biotechnol. 23 (2005) 492.
[31] J.L. Humm, D.E. Charlton, Int. J. Radiat. Oncol. Biol. Phys. 17 (1989) 351.
[32] S. Ftáčniková, R. Böhm, Radiat. Prot. Dosim. 92 (2000) 269.
[33] J.L. Humm, R.W. Howell, D.V. Rao, Med. Phys. 21 (1994) 1901.
[34] J.G. Kereiakes, D.V. Rao, Med. Phys. 19 (1992) 1359.